The influence of flanges on the in-plane seismic performance of URM walls in New Zealand buildings

A.P. Russell & J.M. Ingham

The University of Auckland, Auckland, New Zealand.

2010 NZSEE Conference

ABSTRACT: The influence of flanges (return walls) on the in-plane lateral behaviour of unreinforced masonry (URM) walls is reported. Experimentation was conducted on clay brick masonry walls designed to replicate typical New Zealand construction in the early 20th Century and with flanges of different lengths and at different locations. Testing of URM walls showed that the presence of flanges has a significant effect on the in-plane response of the wall.

The results of experimentation were compared with analytical results determined from previous research, with a high level of correlation. Consequently, it was concluded that the existing analytical model was suitable for determining the response of walls with flanges responding in-plane. Drift limits are also proposed, depending on the in-plane wall failure mode.

1 INTRODUCTION

Many unreinforced masonry buildings in New Zealand can be expected to perform poorly in an earthquake. The construction of such buildings was common in the early part of the 20th Century, but design philosophies were focused on gravity loading, with little thought given to the lateral force resistance of URM walls. Consequently many URM buildings form a significant part of both New Zealand's heritage building stock and that group of buildings which are considered potentially earthquake prone.

Research has been previously presented on in-plane URM wall response, but it has been identified in the literature (see Moon et al., 2006; Yi et al., 2006a,b, 2008) that codified equations for assessing the strength and displacement capacity of walls are overly conservative, particularly when assessing URM walls with flanges (return walls) at either or both ends. Consequently, the objective of this research was to investigate the response of flanged URM walls, in the context of previous research considering failure modes, and to determine strength and displacement limits.

2 BACKGROUND

Yi et al. (2008) noted that previous experimental research at the structural level highlighted the effects of transverse walls (flanges) on the response of in-plane walls and indicated the potential for flanges to influence pier failure modes and maximum strength (Costley, 1996; Moon et al., 2006; Paquette and Bruneau, 2003; Yi et al., 2006b). Yi et al. (2008) also noted that that no experimental data were available which specifically investigate flanged URM walls.

Experiments conducted by Moon (2004) and Yi et al. (2006a,b) suggested that substantial flange participation was observed for in-plane walls in each loading direction in a full scale URM test structure. Flanges were defined by Moon et al. (2006) as the portion of the out-of-plane wall that participates with the in-plane wall to resist lateral loads.

Following full scale testing of a two storey URM building (Moon, 2004; Yi, 2004) where significant flange participation was observed, Yi et al. (2008) developed an analytical model to investigate the

effects of flanges on the behaviour of individual non-rectangular section URM piers. In the absence of experimental data to validate the model, Yi et al. (2008) presumed an example wall and from a pushover analysis, determined that compared to a similar wall with no flanges, the lateral strength could be expected to be greater. It was also determined that the limiting drift is different when the flange is at different locations in relation to the in-plane wall. When the flange is at the toe of the wall (i.e. the flange is in compression) the flange reduces the compressive stress at the toe, and delays toe crushing failure. Conversely, when the flange is at the heel (i.e. in tension) the compressive stress in the toe increases due to the increased weight of the flange. It was determined by Yi et al. (2008) that the location of the flanges has a significant effect on the diagonal tension strength of the wall. If the flange is in the middle of the in-plane wall, it has no effect on the diagonal tension strength, but when the flange is positioned closer to either end of the wall the diagonal tension strength decreases first and then increases.

3 ANALYTICAL MODELS FOR PREDICTING IN-PLANE WALL BEHAVIOUR

The models for determining the behaviour of walls responding in-plane, when including the influence of flanges, are summarised in Equations (1) – (4), which are reproduced from Yi et al. (2008).

$$V_s = \frac{\mu N + 3a_i b_w v_{me}}{1 + \frac{3h_{eff} b_w v_{me}}{N}} \tag{1}$$

$$V_{tc} = \frac{N}{h_{eff}} l_w \left(\frac{a_i}{l_w} - \frac{2}{3} \frac{N}{\beta f_m l_w b_w} \right) \tag{2}$$

$$V_{dt} = b_w l_w b f_{dt} \sqrt{1 + \frac{f_m}{f_{dt}}} \frac{\left(1 + \frac{W_f}{W_w}\right)\left(\frac{1}{6}\left(1 + \frac{W_f}{W_w}\right) + \frac{1}{2}\frac{W_f}{W_w}\right)}{\left(\frac{W_f}{W_w} + \frac{1}{2}\right)^2} \tag{3}$$

$$V_r = \frac{N}{h_{eff}} \frac{\left(\frac{l_w b_w a_i}{2} - \frac{l_w^2 b_w}{6} + (a_i - a_f) A_f \left(1 - \frac{a_f}{l_w}\right)\right)}{\left(\frac{l_w b_w}{2} - A_f\right)} \tag{4}$$

where V_s, V_{tc}, V_{dt} and V_r are the lateral strength of the URM wall corresponding to sliding, toe crushing, diagonal tension and rocking, respectively, a_i is the distance between inertia centre and compression edge of wall, a_f is the distance between centre of flange and compression edge of wall, A_f is the cross-sectional area of the flange, W_w is the weight of the in-plane wall, W_f is the weight of the flange, β is a factor to account for nonlinear vertical stress distribution and has a value $\beta = 1.3$ from Yi et al. (2005), μ is the coefficient of friction, N is the axial load (in terms of force), b_w is the thickness of the in-plane wall (web), v_{me} is the cohesive strength of masonry bed joint, h_{eff} is the effective height of the wall, l_w is the length of the wall, f_m is the axial compressive stress (in terms of stress), b is a factor to account for wall aspect ratio, and f_{dt} is the diagonal tension strength of the masonry.

4 EXPERIMENTAL PROGRAMME

4.1 Wall Specifications

Six walls were constructed and tested, and are termed Walls A3, A3a, A5, A6, A7 and A8. All in-plane walls and flanges were two leaves (240 mm) thick ($b_f = b_w = 240$ mm). Wall A3 was 2000 mm long and 2000 mm high, with an aspect ratio of 1:1. At the conclusion of testing Wall A3, it was

observed that damage was confined to the top nine courses. It was decided that the uncracked material could be utilised as another wall test. The nine courses where damage had occurred in the test of Wall A3 were removed and Wall A3a was thus fifteen courses high with the same length and flange properties as Wall A3, and with an in-plane wall aspect ratio of 1:1.6. Walls A5 – A8 were all 4000 mm long and 2000 mm high, with an aspect ratio each of 1:2.

Table 1: Wall specifications

Wall	b_w	h	l_w	f'_m	c	μ	f_m	f_m/f'_m
	mm	mm	mm	MPa	MPa	MPa	MPa	%
A3	230	2000	2000	18.1	0.4	0.7	0.01	0.055
A3a	230	1200	2000	18.1	0.4	0.7	0.022	0.123
A5	230	2000	4000	10.1	0.1	0.7	0.022	0.220
A6	230	2000	4000	9.2	0.1	0.7	0.041	0.441
A7	230	2000	4000	11.9	0.1	0.7	0.056	0.468
A8	230	2000	4000	9.1	0.1	0.7	0.052	0.576

The axial load on the wall specimens was applied through post-tensioning tendons near the ends of the wall. The axial load on Wall A3a was 22 kN, corresponding to 22 kPa. The axial load on Wall A5 was the same as for Wall A4 (30 kN), but because of the increased cross-sectional area of the wall due to the presence of flanges, this corresponded to an axial stress of 22 kPa. Initially the axial load on Wall A6 was the same as on Wall A5, but at the commencement of testing it was observed that the steel channel used to apply the lateral force was lifting off, and consequently the axial load on Wall A6 was increased to 73 kN, and corresponded to an axial stress of 41 kPa. Similarly, the axial load on Walls A7 and A8 was 76 kN and 71 kN, corresponding to an axial stress of 56 kPa and 52 kPa, respectively. See Table 1.

Details of the flanges are listed in Table 2. Walls A3, A3a and A5 had flanges at both ends with a length of 480 mm on either side of the in-plane wall, with a total flange length of 1200 mm. Walls A6 and A7 had flange lengths of 960 mm on either side of the in-plane wall, with a total flange length of 2160 mm. The flanges were positioned at both ends in the case of Wall A6, and at one end in the case of Wall A7. Wall A8 had flanges at both ends, but on a single side only, and the flanges had a length of 960 mm on the side of the in-plane wall.

Table 2: Flange details

Wall	b_f	l_f	Flanges at	
	mm	mm		
A3	230	1200	both ends	both sides
A3a	230	1200	both ends	both sides
A5	230	1200	both ends	both sides
A6	230	2160	both ends	both sides
A7	230	2160	one end	both sides
A8	230	1200	both ends	one side

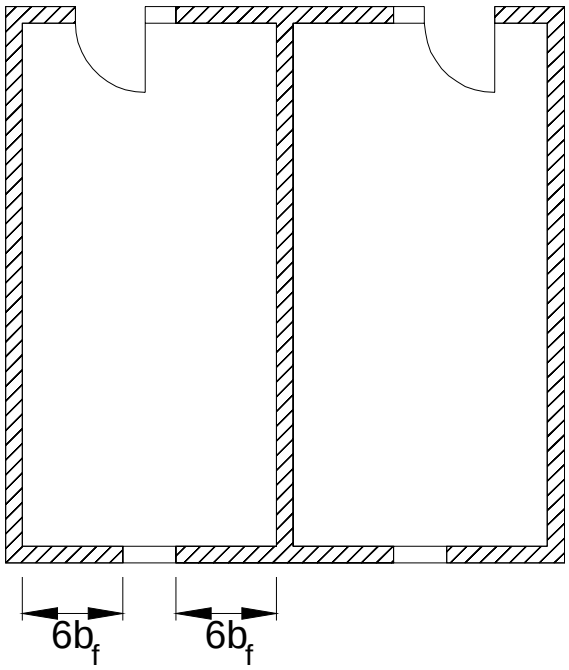

Figure 1: Effective flange lengths (plan view of general URM building)

The effective length of flanges can be determined according to MSJC (2008) or Standards New Zealand (2004), but in this article the definition from MSJC is utilised. According to MSJC (2008), the effective flange length is $6b_f$ on either side of the in-plane wall. For all walls reported in this article, $b_f = 240$ mm, and the effective flange length on either side of the in-plane wall was 1440 mm (see Figure 1). According to these definitions, the length of the flanges on all walls reported in this article were considered to be less than their maximum effective length.

4.2 **Wall Construction**

The walls were constructed with a common bond pattern and with 1:2:9 mortar (cement:lime:sand, by volume), corresponding to ASTM type 'O' mortar, and with nominally 10 mm thick mortar joints. There were header bricks every 4th course. It was intentionally decided to construct the walls in a way that replicated the observed, often deteriorated, finished quality of walls in real New Zealand URM buildings.

4.3 **Test Setup and Instrumentation**

The typical wall setup is shown in Figure 2. The walls were loaded laterally by means of a hydraulic actuator reacting against the laboratory strong wall. A steel channel (referred to here as the "loading beam") was mortared to the top of the wall, and the lateral forces were transferred through plates welded to the underside of the loading beam. The plates extended approximately 100 mm below the loading beam, and thus the applied horizontal force was transferred into the wall through friction on the top surface and also directly into the top course of the wall. This arrangement is typical for pseudo-static wall tests at The University of Auckland and is also representative of tests reported in literature.

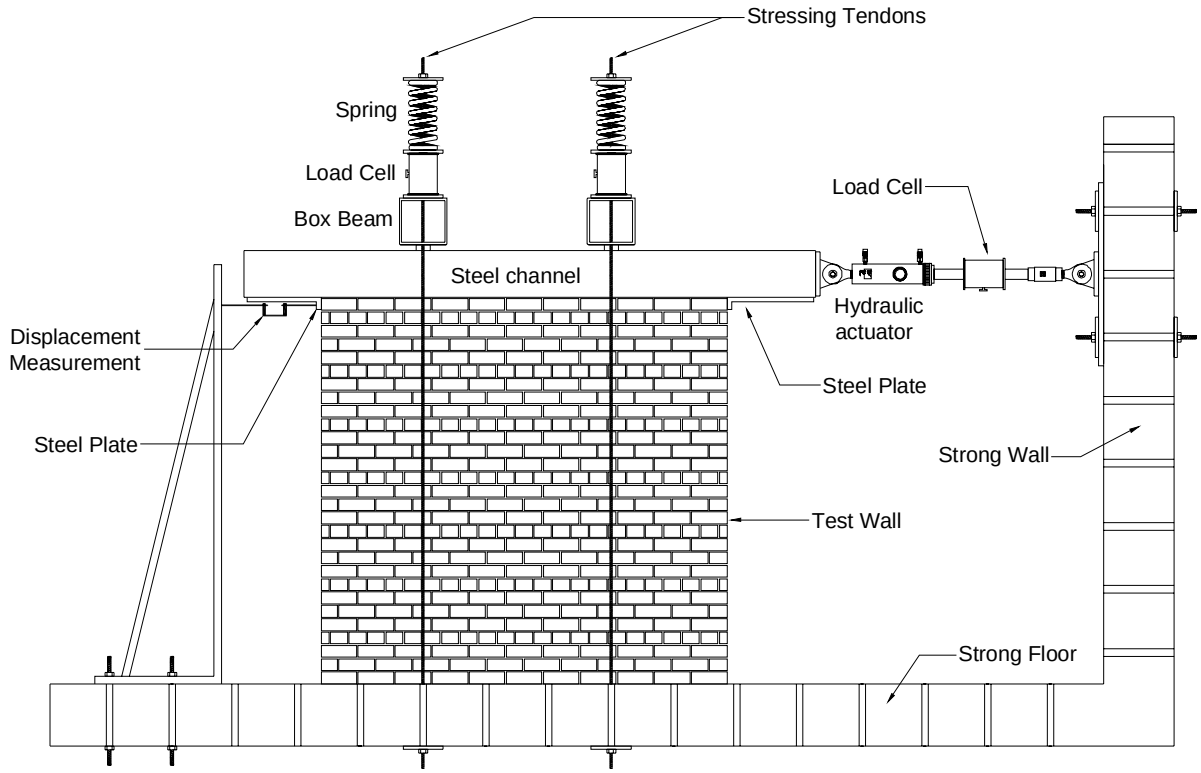

Figure 2: Test setup

4.4 **Predicted Flexural and Shear Strength**

The model proposed by Yi et al. (2008) was used to determine the nominal lateral strength of each of the walls reported in this article. The predicted strengths are shown in Table 3. The maximum nominal shear strength V_n is given as the lowest of the strength limits, and is shown in bold text in Table 3. The model developed by Yi et al. (2008) assumed a single flange, with the location determining a_f (the distance between centre of flange and compression edge of wall) and a_i (the distance between inertia centre and compression edge of wall). Apart from Wall A7, all the walls reported in this article had flanges at both ends, such that $a_i = l_w/2$. For symmetrical walls with flanges at both ends, it was also determined that $a_f = 2a_i$, so that $a_f = l_w$. For Wall A7 in the push cycle (positive) the flange was in compression and $a_f = 0$, $a_i = l_w/3$. When the flange is at the toe of the wall (i.e. the flange is in compression) the flange reduces the compressive stress at the toe, and tends to increase the flexural strength (rocking/toe crushing). For Wall A7 in the pull direction the flange was in tension and $a_f = l_w$, $a_i = 2l_w/3$. In this case, the diagonal tension strength was increased due to the weight of the tension flange, and because of the discontinuous shear stress distribution at the junction of the flange and the in-plane wall (see Yi et al., 2008, for further details).

The model developed by Yi et al. (2008) predicted that for Wall A3, sliding/rocking response could be expected, and that for Wall A3a the limiting strengths due to diagonal tension and sliding were similar, such that a sliding shear/diagonal tension failure was predicted. It was determined that diagonal tension would be the failure mode for Walls A5, A6 and A8. When the flange was in tension in Wall A7 it was predicted that toe crushing would limit the strength, although the limiting strengths due to diagonal tension and rocking were similar, and consequently it was determined that a shear failure or rocking response could be predicted. When the flange was in compression in Wall A7 it was predicted that diagonal tension would limit the strength, although the limiting strength due to sliding was also similar, and consequently a sliding shear/diagonal tension failure was predicted. In Table 3, $A7_t$ refers to Wall A7 when the flange was in tension, and $A7_c$ refers to Wall A7 when the flange was in compression.

Table 3: Predicted wall strengths from model developed by Yi et al. (2008)

Wall	V_s	V_{tc}	V_{dt}	V_r	V_n
	kN	kN	kN	kN	kN
A3	31.7	35.4	57.1	**31.4**	**31.4**
A3a	**45.6**	57.3	45.8	50.9	**45.6**
A5	72.0	136.6	**63.9**	113.7	**63.9**
A6	99.4	222.3	**75.4**	185.4	**75.4**
$A7_t$	80.7	**75.0**	76.1	76.2	**75.0**
$A7_c$	60.4	151.2	**59.3**	89.7	**59.3**
A8	98.4	218.7	**75.0**	182.4	**75.0**

5 EXPERIMENTAL RESULTS

General results are presented in Table 4, where V_n is the nominal shear strength as predicted by the model proposed by Yi et al. (2008), V_{max} is the maximum recorded lateral force, $d_{V,max}$ and $\theta_{V,max}$ are the corresponding displacement and drift, respectively, at V_{max}, V_{crack} is the lateral force when cracking was first observed, θ_{crack} is the drift corresponding to V_{crack}, and d_u and θ_u are the lateral wall displacement and drift, respectively, corresponding to the point at which the lateral force had degraded to 80% of V_{max}, where $\theta_u = d_u/h_{eff}$.

5.1 Force-Displacement Response

The force-displacement response of Walls A3, A3a, A5, A6, A7 and A8 is presented in Figure 3. Walls A3 and A3a failed at a low displacement of 0.02% and 0.01% respectively. Wall A5 also failed at a low displacement of 0.05%. The large peak and subsequent sudden drop in strength observed in the response of Wall A3 corresponded to when the compression flange cracked. After this cracking occurred, the flange was no longer connected to the wall and did not participate in the lateral force resistance. The response of Walls A3 and A5 was not observed beyond a drift of 0.2% and 0.07% respectively, and consequently the post-peak lateral force-displacement response could not be reported.

Table 4: Results

Wall	V_n	V_{max}	V_n/V_{max}	$d_{V,max}$	$\theta_{V,max}$	V_{crack}	θ_{crack}	d_u	θ_u	Behaviour
	kN	kN		mm	%	kN	%	mm	%	
A3	31.4	54.9	0.57	0.6	0.03	54.9	0.02	0.3	0.02	Diagonal tension
A3a	45.6	72.5	0.63	0.8	0.06	72.5	0.01	0.1	0.01	Diagonal tension
A5	63.9	66.0	0.97	0.5	0.03	66.5	0.02	1.0	0.05	Diagonal tension
A6	75.4	66.8	1.12	7.8	0.39	46.4	0.04	19	0.95	Diagonal tension
$A7_t$	75.0	75.0	1.00	2.8	0.14	34.5	0.03	10	0.75	Diagonal tension
$A7_c$	60.4	61.9	0.98	7.7	0.38	34.7	0.03	15	0.50	Diagonal tension
A8	75.0	66.9	1.12	3.6	0.18	60.0	0.06	19.2	0.96	Diagonal tension

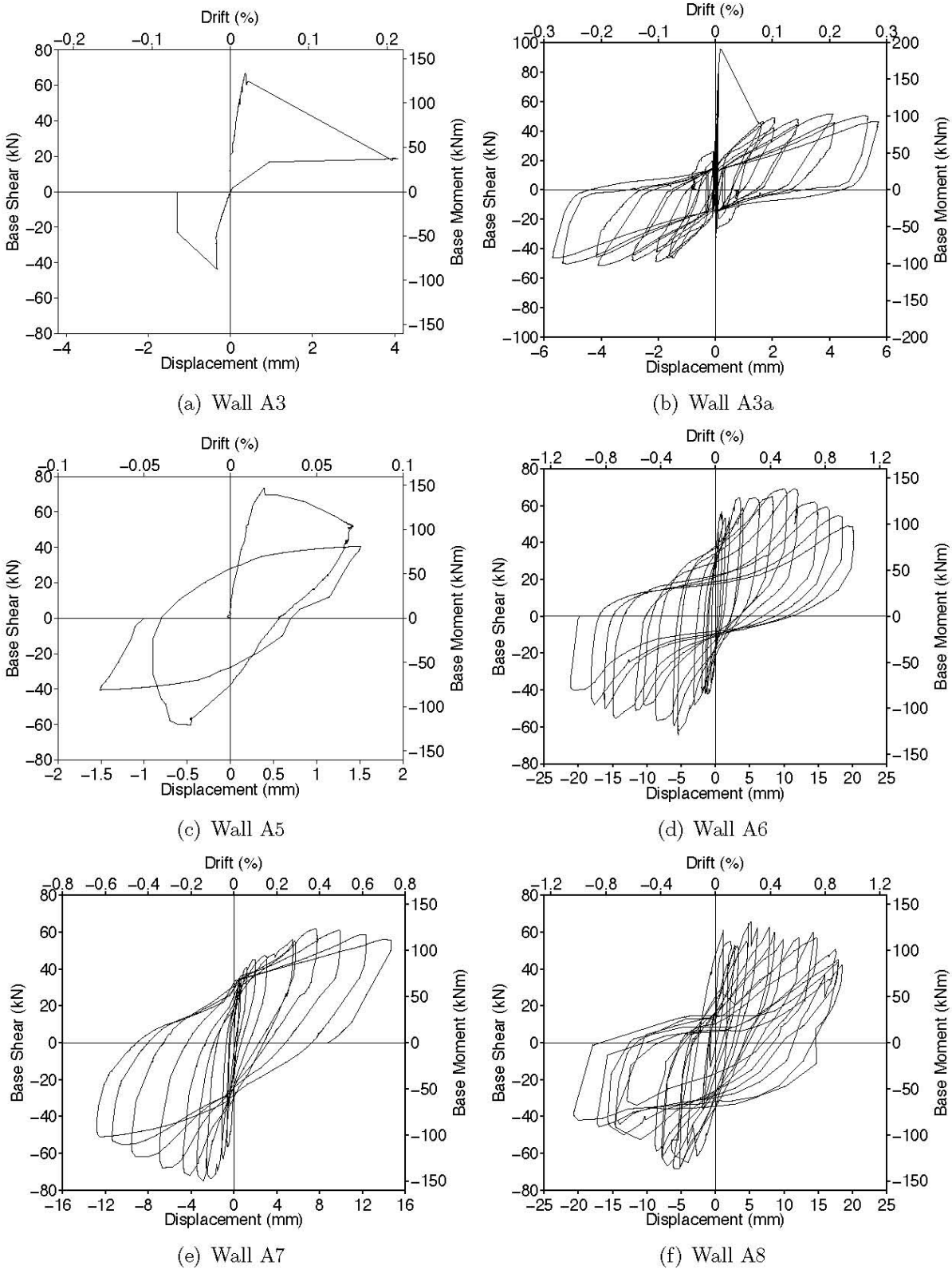

Figure 3: Force-displacement response

Walls A6, A7 and A8 exhibited diagonal tension failure also (see Figure 4), but further hysteretic loops were obtained from these tests. It can be seen that for walls with an aspect ratio of 1:2 and flanges with $l_t = 4b_f$ on each side of the in-plane wall, loss of lateral strength was not sudden and there was some observable strength degradation after the peak lateral force was obtained.

Wall A6 reached a drift of 0.39%, corresponding to the peak lateral force, and an ultimate drift of 0.95% corresponding to $0.8V_{max}$. Similar to Wall A6, Wall A8 exhibited an ultimate drift of 0.96%, which was larger than the drift corresponding to V_{max} (0.18%). This indicates that for a diagonal tension controlled in-plane wall, there can be some residual displacement capacity beyond the suggested drift limit of 0.4%.

The response of Wall A7 was not symmetrical, as was expected due to the non-symmetrical geometry of the wall (see Figure 3(e)). The ultimate drift capacity in the push direction (flange in compression) was 0.5% and in the pull direction (flange in tension) was 0.75%.

(a) damage at conclusion of Wall A5 test

(b) diagonal tension cracking in Wall A7 (flange in tension)

Figure 4: Wall cracking

5.2 **Ultimate Drift**

All the walls reported in this article failed by diagonal tension cracking, which is a shear dominated response. Priestley et al. (2007) suggest a drift limit of 0.4% for walls failing in a shear dominated response. Walls A3, A3a and A5 reached an ultimate drift θ_u of 0.02%, 0.01% and 0.05% respectively, all significantly less than 0.4%. Although testing of Wall A3 was terminated due to concerns about the stability of the axial load blocks on top of the wall, the gravity load carrying capacity of Wall A3 was not actually compromised, and further testing would have been necessary in order to confirm the drift corresponding to collapse. Similarly, for Wall A3a, although the lateral force degraded to $0.8V_{max}$ at a drift of 0.02%, displacement capacity and gravity load capacity was available up to a drift of 0.3%, when the test was terminated. The drift corresponding to collapse and loss of gravity load carrying capacity was not definitively obtained. The only wall where some indication that gravity load carrying capacity was compromised was Wall A5, where bricks became unstable in the top course at the centre of the in-plane wall. The wall as a whole did not lose gravity load carrying capacity.

Walls A6, A7 (in both directions) and A8 all attained an ultimate drift θ_u in excess of 0.4%, and did not lose gravity load supporting capacity. The ultimate drift of Wall A6, A7 (flange in tension), A7 (flange in compression) and A8 was 0.95%, 0.75%, 0.50% and 0.96% respectively.

From the results of Walls A6 – A8, an ultimate drift limit of 0.4% can be confirmed (from the results of Walls A3 – A5, further testing would have been required to confirm this drift limit). Consequently a drift limit of 0.4% for flanged walls with an in-plane wall aspect ratio of 1:2 is recommended.

5.3 **Predicted Behaviour and Measured Behaviour**

Table 4 shows the predicted nominal shear strength V_n as determined by the model developed by Yi et al. (2008), the maximum shear strength V_{max} attained during testing, and the shear strength corresponding to first cracking V_{crack}. The average ratio of V_n/V_{max} was 0.91, with a COV of 24%. For

all the walls, the COV is high, but if the walls with an aspect ratio of 1:2 (Walls A5 – A8) only are considered, then the average ratio is 1.04 with a COV of 7%, indicating a high level of accuracy in the model by Yi et al. (2008).

There was a particularly high level of accuracy in the model when determining the limiting shear strengths of Wall A7 when the flange was both in tension and in compression. Because the model by Yi et al. (2008) was developed for walls with a single flange (at any position on the in-plane wall) it seems reasonable to expect this accuracy. Moreover, for walls with an aspect ratio of 1:2, the model was also particularly accurate, although the predicted strength of Walls A6 and A8 was 12% higher than the measured strength.

Table 5: Comparison of predicted strength accounting for and neglecting flanges

Wall	$\mathbf{V_n}$ kN	$\mathbf{V_{max}}$ kN	$\mathbf{V_n/V_{max}}$	$\mathbf{V_n}$ kN	$\mathbf{V_{max}}$ kN	$\mathbf{V_n/V_{max}}$
	Yi et al. model			NZSEE expressions		
A3	31.4	54.9	0.57	53.0	54.9	0.96
A3a	45.6	72.5	0.63	53.0	72.5	0.73
A5	63.9	66.0	0.97	53.0	66.0	0.80
A6	75.4	66.8	1.12	53.0	66.8	0.79
$A7_t$	75.0	75.0	1.00	53.0	75.0	0.71
$A7_c$	60.4	61.9	0.98	53.0	61.9	0.86
A8	75.0	66.9	1.12	53.0	66.9	0.79
Mean			0.91			0.81
COV			24%			10%

Table 5 shows the comparison between the predicted strength and measured strength, using both the analytical model proposed by Yi et al. (2008) which takes the influence of flanges into account, and also the expressions available in the NZSEE guidelines (2006), which were developed for in-plane piers without flanges. As stated above, for walls with an aspect ratio of 1:2, the model by Yi et al. is particularly accurate, with a mean of 1.04 and COV of 7%. When using the NZSEE equations, the mean of the ratio of the predicted strength to the measured strength is 0.81, with a COV of 10%, indicating that on average, the walls are 19% stronger than predicted. This is an indication of the conservatism inherent in the performance assessment of in-plane URM walls when neglecting the influence of flanges.

Consequently, the model proposed by Yi et al. (2008) is suggested as a more accurate estimation of the strength of flanged in-plane URM walls.

6 CONCLUSIONS

It is concluded that walls with flanges can sustain higher levels of lateral force than walls without flanges, when taking into account the wall aspect ratio and axial load. The influence of flanges must be taken into account when assessing the capacity of in-plane walls to withstand lateral forces generated by earthquakes.

All the walls reported in this article failed in diagonal tension (shear dominated response). The limiting drift of 0.4% was suggested in the literature as the ultimate drift capacity of in-plane walls where the response was dominated by force-controlled actions. The tests reported in this article confirmed that this is a suitable drift limit, and θ_u = 0.4% for walls failing in diagonal tension is

recommended, with the proviso stated above.

The model proposed by Yi et al. (2008) was verified against Walls A5 – A8 with a high level of correlation. Consequently, it is recommended that when assessing the in-plane response of flanged URM walls, the model by Yi et al. (2008) is used.

REFERENCES:

Costley, A. C. (1996). Dynamic Response of Unreinforced Masonry Buildings with Flexible Diaphragms. NCEER-96-0001. University of Buffalo, Buffalo, NY, (PB97-133573, MF-A03, A15).

Magenes, G. and Calvi, G. M. (1997). "In-plane seismic response of brick masonry walls". Earthquake Engineering & Structural Dynamics, 26(11):1091–1112.

Moon, F. L. (2004). Seismic Strengthening of Low-Rise Unreinforced Masonry Structures with Flexible Diaphragms. PhD thesis, Georgia Institute of Technology, Atlanta, GA, USA.

Moon, F. L., Yi, T., Leon, R. T., and Kahn, L. F. (2006). "Recommendations for Seismic Evaluation and Retrofit of Low-Rise URM Structures". Journal of Structural Engineering, 132(5):663–672.

MSJC (2008). Building Code Requirements for Masonry Structures (TMS 402/ACI 530/ASCE 5). American Concrete Institute; Structural Engineering Institute; The Masonry Society (Masonry Standards Joint Committee), Boulder, CO, USA.

NZSEE (2006). Assessment and Improvement of the Structural Performance of Buildings in Earthquakes. Recommendations of a NZSEE Study Group on Earthquake Risk Buildings. New Zealand Society for Earthquake Engineering.

Paquette, J. and Bruneau, M. (2003). "Pseudo-dynamic testing of unreinforced masonry building with flexible diaphragm". Journal of Structural Engineering, 129(6):708– 716.

Priestley, M., Calvi, G., and Kowalsky, M. (2007). Displacement-Based Seismic Design of Structures. IUSS Press : Fondazione Eucentre, Pavia, Italy.

Standards New Zealand (2004). NZS 4230:2004, Design of Reinforced Concrete Masonry Structures. Standards New Zealand, Wellington, New Zealand.

Yi, T. (2004). Experimental Investigation and Numerical Simulation of an Unreinforced Masonry Structure with Flexible Diaphragms. PhD thesis, Georgia Institute of Technology, Atlanta, GA, USA.

Yi, T., Moon, F. L., Leon, R. T., and Kahn, L. F. (2005). "Effective Pier Model for the Nonlinear In-Plane Analysis of Individual URM Piers". The Masonry Society Journal, 23(1):21–35.

Yi, T., Moon, F. L., Leon, R. T., and Kahn, L. F. (2006a). "Analyses of a Two-Story Unreinforced Masonry Building". Journal of Structural Engineering, 132(5):653–662.

Yi, T., Moon, F. L., Leon, R. T., and Kahn, L. F. (2006b). "Lateral Load Tests on a Two-Story Unreinforced Masonry Building". Journal of Structural Engineering, 132(5):643–652.

Yi, T., Moon, F. L., Leon, R. T., and Kahn, L. F. (2008). "Flange Effects on the Nonlinear Behaviour of URM Piers". The Masonry Society Journal, 26(2):31–42.